Energy 55 (2013) 529–540

Contents lists available at SciVerse ScienceDirect

Energy

journal homepage: www.elsevier.com/locate/energy

Assessment of CO_2 injection into the south Utsira-Skade aquifer, the North Sea, Norway

V.T.H. Pham [a,*], F. Riis [a], I.T. Gjeldvik [a], E.K. Halland [a], I.M. Tappel [a], P. Aagaard [b]

[a] Norwegian Petroleum Directorate (NPD), Pb600, 4003 Stavanger, Norway
[b] Department of Geosciences, University of Oslo, 0316 Oslo, Norway

ARTICLE INFO

Article history:
Received 24 October 2012
Received in revised form
5 March 2013
Accepted 6 March 2013
Available online 24 April 2013

Keywords:
CO_2 storage
Sequestration
Compositional simulation
Utsira
Aquifer

ABSTRACT

To estimate the capacity of CO_2 storage in a southern part of Utsira/Skade aquifer, a reservoir model was built to simulate the long-term behavior of CO_2 injection. The model covers 1600 km^2 in the southern part of the Norwegian sector. The study illustrates potential migration and to forecast possible migration of CO_2 from the Skade Formation into the Utsira Formation above. CO_2 from Skade sand can penetrate through a clay layers into Utsira sand if the clay between Skade sand and Utsira sand has permeability from 0.1 mD and higher. About 170 Mt (million tonne) CO_2 can be injected in Utsira sand in the segment model with 4 horizontal wells over 50 years, BHP (bottom-hole pressure) change of 10 bars, no water production. After 8000 years of storage, the dissolved part is nearly 70%, residual trapping is less than 1% and mobile CO_2 has decreased to 29% of total amount of injected CO_2. These results are based on a residual saturation of CO_2 of 0.02. If a residual saturation of CO_2 is 0.3, CO_2 trapped by residual mechanisms is 13% of total CO_2 injected after 8000 years. Mineral trapping by geochemical reactions was not considered in the simulation, but will add additional storage capacity.

1. Introduction

Underground storage of carbon dioxide is proposed as a greenhouse-gas mitigation option by reducing the release rate of CO_2 to the atmosphere [1,2]. CO_2 injected underground can be stored in reservoirs by four trapping mechanisms: structural/stratigraphic, residual, dissolution and mineral trapping [3]. In the short-term, normally the three mechanisms structural, residual and dissolution trapping dominate, while dissolution and mineral trapping become more important in the long term [4]. One important type of storage reservoir is saline aquifers, which have too high salinities to be used for irrigation and domestic water supply. These can handle large volume of CO_2, they commonly have thick successions of tight clay or shale cap-rocks, and they are often associated with petroleum exploration and production with infrastructure capable of CO_2 storage development. Offshore saline aquifers have additional advantages because they are located far away from land-based settlements that could potentially be harmed by CO_2 leakage.

Subsurface storage of CO_2 has a long history on the Norwegian continental shelf. CO_2 storage has been carried out in the Sleipner Field (North Sea) since 1996 [5] and in the Snøhvit Field (Barents Sea) since 2008 [6]. Several studies have established the large carbon storage potential on the Norwegian continental shelf, especially in deep saline aquifers. During the last two years, the Norwegian Petroleum Directorate (NPD) has interpreted relevant data on the Norwegian continental shelf in order to classify potential sites for CO_2 storage. The CO_2 storage atlas for the Norwegian North Sea has indicated possible storage sites, and estimated storage capacity.

The Utsira Formation and the underlying Skade Formation are considered to be a single aquifer that comprises parts of a large Miocene-Pliocene sandy deltaic complex. This deltaic complex is located in the UK and Norwegian sector in the northern North Sea. The Utsira/Skade aquifer is one of 10 aquifers which was evaluated as suitable for CO_2 storage in the northern North Sea by Halland et al., [7]. This aquifer has porous and permeable sands, ideal depth levels for storing fluid CO_2 (700–3000 m) and good seals. They are located in the northern North Sea, and have the potential for storing giga-tonnes of CO_2. In the Sleipner Field (North Sea) one mega-tonne of CO_2 has been injected per year since 1996 [5,8] NPD has remapped and a calculated the total theoretical storage capacity of the Utsira/Skade aquifer with respect to CO_2 storage [7].

* Corresponding author.
E-mail address: van.pham@npd.no (V.T.H. Pham).

0360-5442/$ – see front matter
http://dx.doi.org/10.1016/j.energy.2013.03.026

The Utsira Formation and the underlying Skade Formation forms the main parts of a large Miocene-Pliocene aquifer related to the sandy deltaic complex located in the UK and Norwegian sector in the northern North Sea [7,9–11].

The purpose of this study was to estimate CO_2 storage capacity and long-term behavior of CO_2 in the Utsira and Skade Formations based on regional reservoir simulations in the southern part of Utsira-Skade aquifer system. The present study was set up to test if large volumes of CO_2 can be injected into the aquifer with a low risk of migration to areas with insufficient seal. A regional reservoir model covering 1600 km^2 of the aquifer system was built to simulate the long-term behavior of CO_2 injection. Additional objectives of the study were to investigate and illustrate potential migration toward the western border of Norwegian sector, and to forecast possible migration of CO_2 from the Skade Formation into the Utsira Formation above. Different scenarios of the communication between the Skade and Utsira Formation were studied in the reservoir simulations, by varying the transmissivity of the mudstone between them. The simulations could constrain the expected injectivity and the amount of CO_2 which can be injected into the formations. Furthermore, the simulation results will also increase our understanding of the distribution of the CO_2 plume in the aquifers and see under what conditions the plume would enter into areas with insufficient seal.

1.1. Previous case study simulations

Valuable lessons have been learned from earlier case-studies of offshore CO_2 storage operations. In the Barents Sea, Estublier and Lackner [12] and Pham et al., [13] investigated the long-term CO_2 behavior at the Snøhvit field and forecasted the CO_2 migration pathways and sealing capacity of main faults over 1000 years. In the northern part of the North Sea, Eigestad et al. [14] reported a study of CO_2 injection in the Johansen Formation. The study investigated the effects of boundary conditions, vertical grid refinement, permeability and grid-block transmissibility data on CO_2 plume migration.

Lindeberg and Bergmo [15] performed numerical modeling to better understand the long-term behavior and distribution pattern of the CO_2 plume in the North Sea Utsira aquifer. At the Sleipner storage site, CO_2 plume behavior has been monitored and calibrated against 4D-seismic data [16]. In the studies, the storage capacity of the entire Utsira Formation has been estimated to be between 20 and 60 Gt (giga tonne) CO_2 [17] and over 42 Gt CO_2 [9]. The storage capacity of the entire Skade Formation was estimated to be about 15 Gt [9]. Singh et al., [18] have suggested that taking into account gravity segregation and/or modifying the simulation input data, could improve the match with observations for black-oil and compositional simulations.

In a study to explore geological storage sites for CO_2, Bergmo et al., 2009 found that 74% of the CO_2 injected into the southern part of Utsira Formation was in aqueous solution and the remaining fraction immobilized after 5000 years. The study concluded that the required 125 million tonnes (Mt) CO_2 could easily be injected into this part of Utsira Formation. For suitable injection points, CO_2 will migrate at most 33 km from the injection point during the 5000 year period and there are no indications that it will migrate to any places where it may reach the shallow parts of the formation in the west [19]. The Utsira Formation thus appears to provide particularly robust CO_2 storage sites.

The reactivity and mineral-trapping potential of the Utsira sand has been investigated by several researchers and found to be rather limited as reactive mineral phases are minor constituents of the reservoir sand [20–23]. However, compared with the dissolved fraction, mineral trapping may be even higher in the long term [20,24]. These studies give an overview of the mineral trapping capacity of the sand in Utsira Formation. Mineral trapping is not included in the present study, thus giving also a conservative estimate of dissolution trapping.

2. Geological overview

In the early Paleocene, major rifting, associated igneous activity and uplift led to the emplacement of oceanic crust (seafloor spreading) between Greenland and the Norwegian Margin [25]. In the study area, the result was deposition of coarse clastics derived from the western margin, forming a series of submarine fans that inter-finger with hemipelagic sediments to the east [25]. The deposition of coarse clastics continued into the Neogene.

The Skade Formation was deposited in the early Miocene as turbidites that cover an area about 26,500 km^2 in Norwegian sector, mainly in the south of the Viking Graben (Fig. 1b). The maximum thickness exceeds 300 m, but average 50–100 m and decreases rapidly towards the east [7,25,26]. Above the Skade Formation, the middle Miocene Eir member sand (informal) was deposited in the western part, while the sand becomes more fine-grained towards the east and middle Miocene mudstones overlie Skade Formation in the eastern part [7]. The porosity and permeability of the Skade Formation is very good. Thin mudstone layers are observed in well logs, but they are not observed on the seismic data due to a resolution of a few meters.

The Utsira Formation is deposited in upper Miocene and lower Pliocene and consists of shallow marine sandstones deposited in a narrow strait with tidal inlet from the Møre basin in the North [25]. The sands of the Utsira Formation display a complex architecture, and the elongated sand body extends some 450 km NS and 90 km WE [7,26,27], Fig. 1a. The central part of Utsira Formation is thinner with possibly more shaly interbeds than in the depocenters. A prograding delta front in Upper Miocene/Lower Pliocene (top Utsira level) is observed [27]. The two major sand depocenters, one in the north and the other in the south, have been mapped out, with thickness up to 400 m [7,28].

The Utsira-Skade aquifer is the distal part of a great Miocene-Pliocene delta-complex originating from the west Shetland Platform [10,11]. In the UK sector the post Eocene sands are called Hutton sands (informal). In the Norwegian sector, the Miocene-Pliocene delta-complex is divided into four units [7], and towards the west there is communication between the units [27]. In the west, there is a sandy unit between the Skade and Utsira Formations. Towards the east, this unit evolves into a mudstone and is assumed to act as a seal between the formations (Fig. 2) [7]. The upper parts of the Miocene-Pliocene delta complex consist of Upper Pliocene sands which locally are buried less than 200 m below sea floor. Details about fluid communication within this huge aquifer are not yet mapped out. The seal overlain the Utsira Formation is Pliocene and Quaternary marine clay stones of the upper part of the Nordland Group. The clay stones are grey, sometimes greenish-grey and grey-brown, soft, sometimes silty and micaceous [9].

The total reservoir rock volume of Utsira/Skade aquifer, that are buried at depths deeper than 700 m and evaluated as suitable for storing CO_2 is estimated to about 2.5×10^{12} m^3, and the pore volume is 5.26×10^{11} m^3 [7].

There is a part of the aquifer with the depth that is the shallower than −700 m under sea lever. This part is in the north – north-west of the simulation model and this part is not considered as suitable place to inject CO_2. But the shallow aquifer part may affect the pressure increase of the model and distribution of CO_2 plume, see Fig. 3.

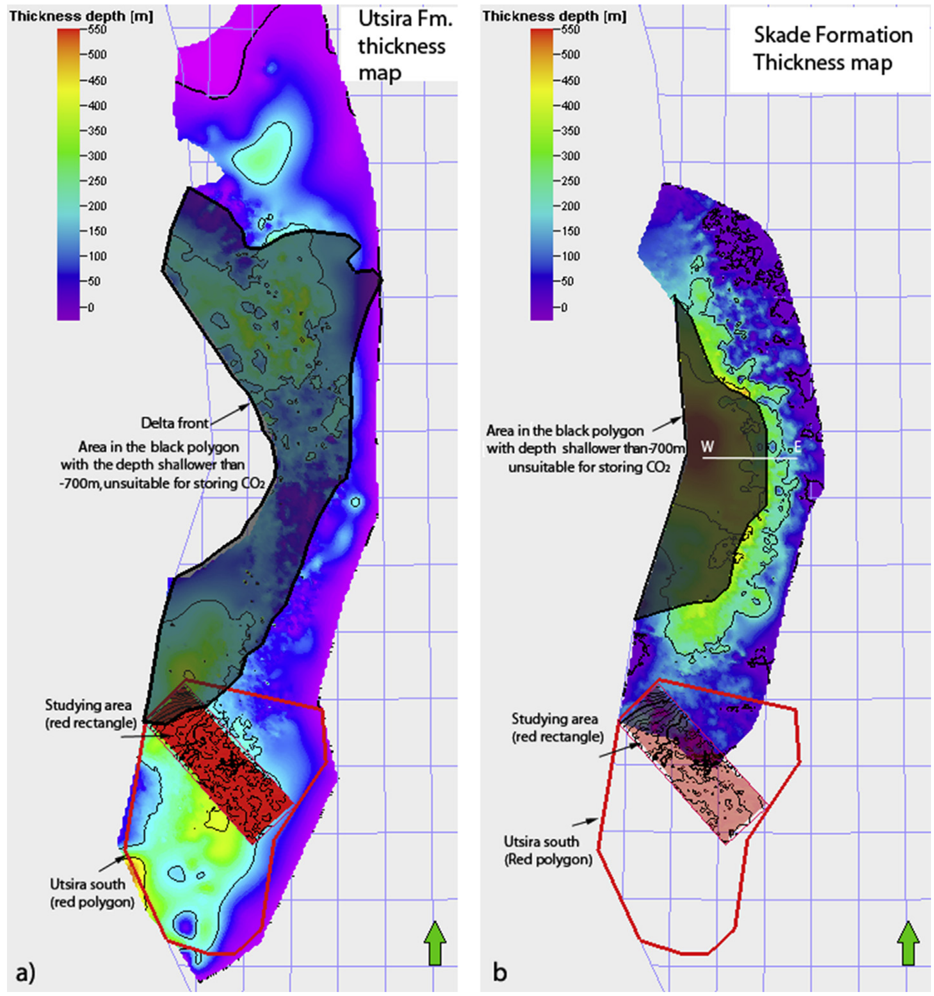

Fig. 1. (a) Utsira Formation thickness map shows the area inside the black polygon (line) and in the left side of the polygon are shallower than −700 m. There are two main thick sand areas (depocenter); one inside the red polygon; smaller one in the north (b) Skade Formation thickness map. The Skade Formation is older than and is under Utsira Formation. The red polygon only covers small part of Skade Formation. The areas inside the black polygon and in the left side of the polygon are shallower than −700 m. (For interpretation of the references to color in this figure legend, the reader is referred to the web version of this article.)

3. The reservoir simulation model

The model area in this study (Fig. 3) was selected as a segment in the southern depocenter of the Utsira Formation (Fig. 1a). The reservoir properties of the Utsira Formation within the segment are typical for this depocenter. The selection of the segment based on the top surface topography is such that the model could include both the migrating direction to the north and also to the west boundary of the segment. The model covers an area of about 1600 km^2. We have applied two grid sizes for the same model; 500 m $\times$ 500 m and finer 200 m $\times$ 200 m to investigate the effect of different grid-size. The pore volume of Utsira/Skade sand in the model is approximately 1.1 $\times$ 10^{11} m^3. Within the model, there is one horizontal injection well in each segment and for each formation. There are two separate injection wells for Utsira Formation and Skade Formation. The location of injection wells are shown in Fig. 3 and injection points are at nearly bottom of the formation sands.

Within the study area, the mudstone layer between two formations covers the whole of area except small local sand injection observed in seismic. The simulation model is set up with two separate horizontal injection wells, one in the Utsira sand and the other in the Skade sand. Reservoir pressure is hydrostatic and the bottom hole pressure could increase 30 bars with depths 900 m and deeper. Bottom-hole pressure was constrained to increase from 10 bars to 15 bars applied for depths from 700 m to 900 m. This constraint is applied because at shallow depths the Utsira sand and the seal do not resist large changes of pressure. The injection period is applied for 50 years and the observation of the plume for about 8000 years after injection stops.

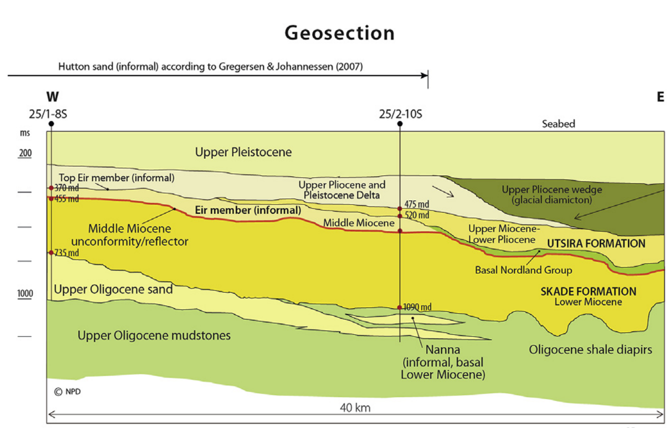

Fig. 2. Geological cross-section [7], the location of the cross-section is displayed in Fig. 1b shows sand–sand connection between Utsira and Skade Formation in the west at shallow depths (between two well 25/1-8S and 25/2-10S).

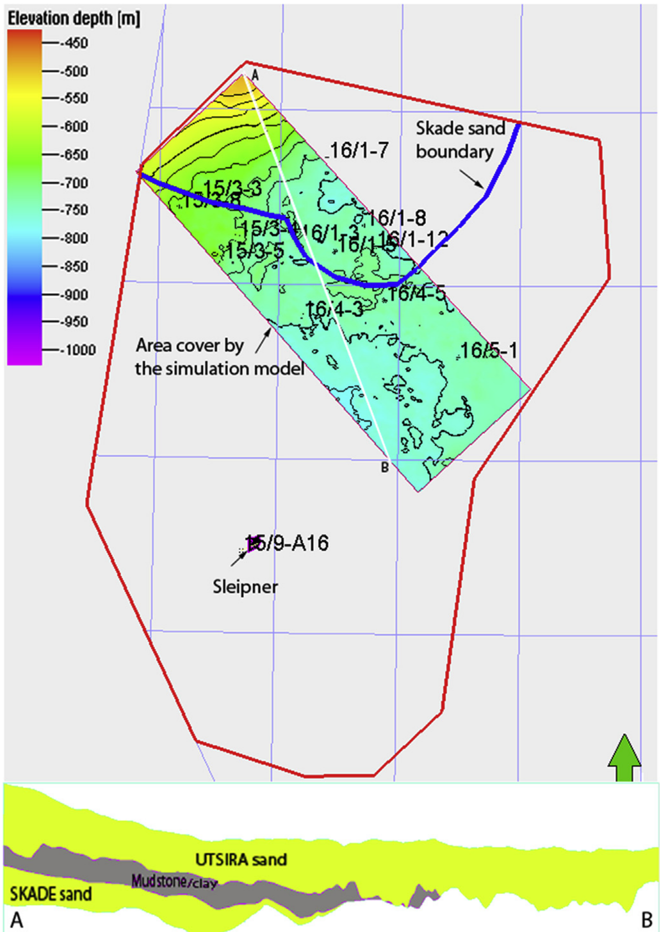

Fig. 3. Upper picture shows studying area inside red rectangle with top Utsira surface covered by simulation model, and cross-section below (AB) was exaggerated vertically. The cross-section shows mudstone layer between two sands; Utsira sand and Skade sand. In the northern and north-western the model contacts with shallower part of the aquifer, the contact displayed by red line on the left of the cross-section below. (For interpretation of the references to color in this figure legend, the reader is referred to the web version of this article.)

3.1. Porosity and permeability

Porosity was calculated based on the density logs, which exist for a few of the relevant wells. These calculations commonly gave porosity values well above 40% which were considered unrealistically high taking into account that unconsolidated sands at surface conditions rarely exceed an average porosity of 40%. There are no core measurements to calibrate the log data. Sonic velocities also suggest high porosity values. In the model it was decided to input porosities in the range of 30–35% for Utsira sand and 32% average for Skade sand. This is considered to be a conservative estimate. Average horizontal permeability is from 0.1 mD for shale/mudstone to 1000 mD for good sand. Net to gross is 0.7 in Ref. [9] and 0.98 [29] and a net to gross value of 0.98 is selected for this model.

Relative permeability curves for brine and supercritical CO_2 phases were obtained from experimental data [18]. The relative permeability curves were calculated to fit Corey's exponent $n = 2.8$ with formation water and CO_2 with irreducible water saturation $S_{wi} = 0.11$ and critical saturation for water 0.386 (at the saturation, flow of the phase ceases), and critical CO_2 saturation 0.02 [18], see Fig. 4 and Table 1. Imbibitions curve is used to estimate amount of CO_2 trapped as residual if critical CO_2 saturation is assumed 0.3; compare Fig. 4.

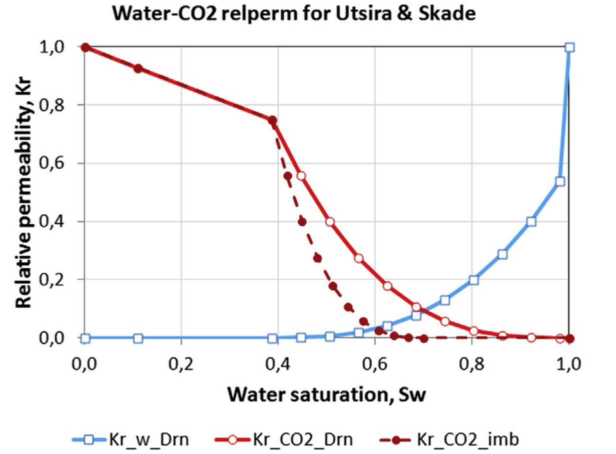

Fig. 4. Relative permeability curves for CO_2 critical and water phase based on data from Ref. [18] and the imbibition curve applied for CO_2 phase, assuming critical saturation of CO_2 is 0.3.

3.2. Formation water

For the water compositional calculations we used the initial NaCl and $CaCl_2$ mol fractions in the reservoir water to correspond to reported formation waters from Egeberg and Aagaard [30] and adjusted in Ref. [22]. Reservoir condition set up at the reference depth of 850 m is at pressure of about 85 bars and a temperature about 37 °C. Parameters used for the model is listed in Table 2.

For the numerical simulations the ECLIPSE300 – compositional simulator was used with the CO2STORE modules that handle CO_2 flow, NaCl and $CaCl_2$ components. Mutual CO_2 solubility in brine is calculated based on Spycher et al., [31], the calculation relied on activity coefficient of H_2O-rich phase and fugacity for CO_2-rich phase and was fitted with experimental data from literature [31,32].

3.3. Summary of all simulation cases

A summary of all simulation cases in the study are listed in Table 3. The base case simulation applied for injection into the Utsira Formation (U200_BASE) assumes homogenous sand and no contact with the shallow aquifer part and the model has a grid size of 200 m × 200 m. The model with the coarser grid (grid size 500 m × 500 m), U500, was simulated to study the effect of grid size. Effect of anisotropy was studied by comparing the isotropic U200_BASE base case ($K_v/K_h = 1$) with U200_VH01 and

Table 1
Relative permeability calculated from data provided from Ref. [18].

For curves generation, drainage			For curves generation, imbibition		
Sw	Kr_w_Drn	Kr_CO2_Drn	Sw	Kr_w_imb	Kr_CO2_imb
0.000	0.000	1.000	0.000	0.000	1.000
0.110	0.000	0.929	0.110	0.000	0.929
0.386	0.000	**0.750**	0.386	0.000	**0.750**
0.445	0.001	0.558	0.417	0.000	0.558
0.505	0.006	0.402	0.449	0.001	0.402
0.564	0.019	0.276	0.480	0.003	0.276
0.624	0.042	0.179	0.512	0.007	0.179
0.683	0.078	0.108	0.543	0.013	0.108
0.742	0.129	0.058	0.574	0.022	0.058
0.802	0.199	0.026	0.606	0.033	0.026
0.861	0.289	0.008	0.637	0.049	0.008
0.921	0.402	0.001	0.669	0.067	0.001
0.980	**0.540**	0.000	0.700	**0.540**	0.000
1.000	1.000	0.000	1.000	1.000	0.000

Bold numbers indicate the end point of the relative permeability.

Table 2
Water composition used for simulation [22].

Component	CO_2	H_2O	NaCl	$CaCl_2$	$CaCO_3$
Mol fraction	0.001	0.951	0.046	0.001	0.001

U200_VH001 cases with vertical vs horizontal permeability ratio of respectively $K_v/K_h = 0.1$ and 0.01 (K_v: vertical permeability and K_h: horizontal permeability). U200_BARRIER case with five internal mudstone layers within the Utsira sand laterally is to test the trapping effectiveness of the internal barriers (U200_BARRIER). Hysteresis was included in the case with homogenous sand (U200_HYSTER) and in the case with internal mudstone layers (U200_BARR_HYS) to estimate CO_2 trapped by residual mechanism when residual CO_2 saturation (or critical saturation for CO_2) was assumed higher.

The base case applied for injection into Skade Formation, S_BASE, is homogenous sand, no aquifer contact with the Utsira Formation, and has a grid size of 500 m × 500 m. Another simulation case with shallow aquifer contacted (see Fig. 3), is the case S_AQUIFER, was done to forecast a pressure build-up scenario. Other cases use different locations of the injection well to test different behaviors of the CO_2 plume. The mudstone between the two formations was assigned various permeability: 0.001, 0.01 and 0.1 mD (in cases S_KTOP0001, S_KTOP001 and S_KTOP01) to investigate in which condition the CO_2 could penetrate through the mudstone into the Utsira sand.

The initial injection rate in one injection well is 19,000 tonnes/day CO_2 (10 million sm^3/day, 1 tonnes of CO_2 is equal 517.6 Sm^3), while the recent injection rate at Sleipner is approximately 2750 tonnes/day (1 Mt/year) (Eiken et al., 2011).

4. Results

4.1. CO_2 injection in the Utsira Formation

The results of base case of CO_2 injection in the Utsira Formation (U200_BASE) and also the case U500, showed that the cumulative CO_2 volumes injected were approximately 113 and 130 Mt, Table 3 (approximately 58,000 and 67,000 million Sm^3in Fig. 5) and for the other cases from 127 to 155 Mt after 50 years with one injection well. With four and five injection wells, the cumulative CO_2 volumes injected increase to 167 and 172 Mt, respectively (Table 3). Injection rate decreased from initial injection rate at 7 Mt/year to 1 Mt/year (10 million Sm^3/day − 1.6 million Sm^3/day in Fig. 5) during 50 year injection period in these two cases. Injection rate decreases due to the bottom-hole pressure (BHP) reaches the constraint. The constraint of BHP for injection in the Utsira sand is 10 bars for the cases, see Table 3. Therefore, the average reservoir pressure increases about 13–15 bars (please see Fig. 5).

The CO_2 injection plume distribution covers over an area with diameter about 12 km at the end of 50 year injection in the U500 case and the U200_BASE base case, (Fig. 6a and b). The distribution area of CO_2 injection plume in the U200_BARRIER case is affected by internal mudstone layers that act as internal barriers to hinder CO_2 migrates upward. In the case U200_BARRIER, the plume could not reach the top of the reservoir after 50 years injection (Fig. 6c).

A general observation of the CO_2 plume after 8000 years after injection shows that the CO_2 migration follows the topography and accumulates up in surrounding local structures. The CO_2 plume distribution is displayed for the two cases U200_BASE and U200_BARRIER (Fig. 7a and b). In both cases, with and without mudstone layer inside the reservoir sand, most of the mobile CO_2 phase migrates up to the top of Utsira Formation at 8000 years after injection. After injection 3000 years, the most of CO_2 migrates to the top of the reservoir in the U200_BARRIER case. The area covering by the CO_2 plume in the U200_BARRIER case (the case is with the internal mudstone layers) is smaller than that in the base case which is without mudstone layers (Fig. 7a and b). The CO_2 is trapped as residual phase or partly trapped structurally underneath the internal mudstone layers. The internal mudstone layers play an important role to trap CO_2 underneath and inside the Utsira sand, which leads to less CO_2 migration to the top of the reservoir, Figs. 6c and 7b.

With the present model, CO_2 could migrate away from the injection well for about 20 km. However, slightly higher slopes could enhance the migration velocity and increase the extent of migration. CO_2 plume did not reach the area at depths shallower than −700 m in the west in all the cases U500, the base case U200_BASE (Fig. 7), and U200_BARRIER, U200_VH01 and U200_VH001 (Fig. 8). Consequently, with suitable well locations (20 km away from the −700 m depth line), the model indicated that large volume of CO_2 can be stored in the Utsira Formation without migrating into areas shallower than 700 m.

The lower vertical permeability could make more difficult for mobile CO_2 to migrate upward to the top and enhance lateral extension of the mobile CO_2. The lateral extension of the CO_2 plume

Table 3
Simulation cases summary, all the case with initial injection rate 10 MSm^3 (unit for injected volume, Mt: million tonnes).

Formation	Grid size model	Simulation cases	Describe	BHP change	Injected vol. Mt
UTSIRA	500 × 500	U500	Homogenous sand, no contact with shallow aquifer part, $K_v/K_h = 1$, 1 injection well	10 bars	113
	200 × 200	U200_BASE	*Base case*, homogenous sand, no contact with shallow aquifer part, $K_v/K_h = 1$, 1 injection well	10 bars	129.8
		U200_VH01	K_v/K_h is 0, 1 injection well	10 bars	136.0
		U200_VH001	K_v/K_h is 0.01, 1 injection well	10 bars	155.6
		U200_BARRIER	5 mud-stone layers inside Utsira sand/internal barrier, 1 injection well	10 bars	153.3
		U200_HYSTER	Same base case and applied hysteresis, 1 injection well	10 bars	127.7
		U200_BARR_HYS	Same U200_BARRIER case and applied hysteresis, 1 injection well	10 bars	127.7
		U200_4WELL	Same U200_BARRIER case and applied hysteresis, 4 injection wells	5/10/15 bars	119.7/166.8/214.7
		U200_5WELL	Same U200_BARRIER case and applied hysteresis, 5 injection wells	10 bars	172.0
SKADE	500 × 500	S_BASE	*Base case*, homogenous sand, no contact with shallow aquifer part, Permeability of the mud-stone (on top Skade Formation) is 0.0001 mD, 1 injection well	30 bars	92.1
		S_KTOP000	Permeability of the mud-stone on top SKADE Formation is 0.001, 1 injection well	30 bars	98.3
		S_KTOP00	Permeability of the mud-stone (on top Skade Formation) is 0.01, 1 injection well	30 bars	121.7
		S_KTOP0	Permeability of the mud-stone (on top Skade Formation) is 0.1, 1 injection well	30 bars	147.9
		S_AQUIFER	Contact with the shallow part of the aquifer, 1 injection well	30 bars	163.7
		S_RELOCATION	New location of injection point	30 bars	187.9

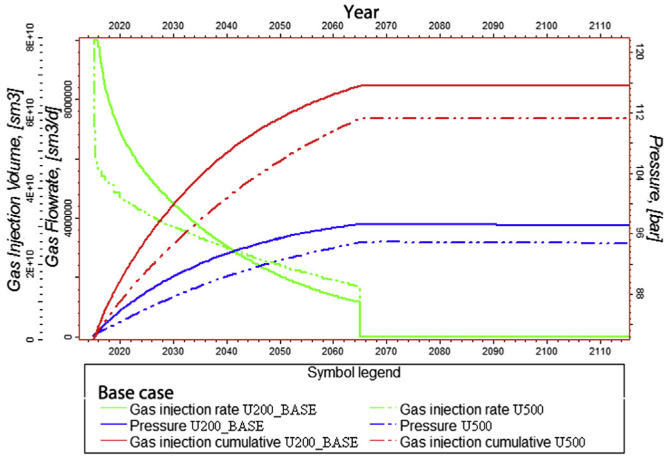

Fig. 5. Base case injection profile in Utsira Fm. (grid size of U500 is 500 m × 500 m and fine grid U200_BASE is 200 m × 200 m).

accelerates dissolution of CO_2 into the brine. In addition, the lower vertical permeability could make also more difficult for CO_2 saturated solution (heavier water) to sink downward. Heavier water or CO_2 saturated solution sinking downward process normally accelerate dissolution of CO_2 in the water. However, this process is prevented will make the CO_2 dissolution process after injection slower and lead to more amount of the mobile CO_2 phase is left. Fig. 8 clearly shows that the CO_2 plume covers a largest area when the sand has lowest vertical permeability, K_v/K_h: 0.01 (Fig. 8a, b and d). The lateral extension is enhanced showed clearly in this case. The CO_2 residual trapping of this case is also higher than the case with higher vertical permeability (Fig. 8c).

4.2. CO_2 injection in the Skade Formation

The simulation result of base case S_BASE shows that the cumulative CO_2 volume injected in Skade sand is approximately 92 Mt (48,000 million Sm^3, Fig. 9) after 50 year injection. Injection rate at the beginning was ca. 19,000 tonnes/day (10 million Sm^3/day) and decrease to approximately 3,800 tonnes/day (2 million Sm^3/day), Fig. 9. The limit change of BHP is constrained for an increase of

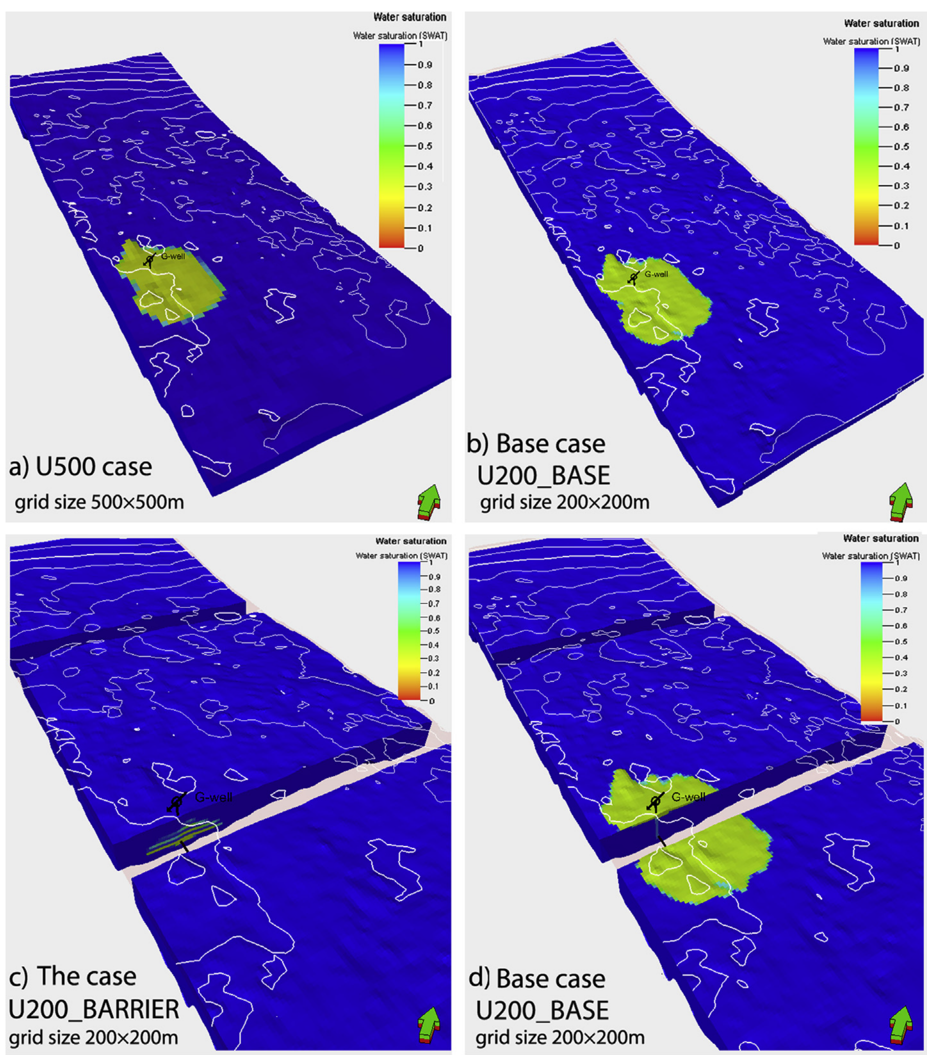

Fig. 6. The CO_2 injection plume observed at the end of 50 years of injection: (a) the U500 base case with grid cell of 500 m × 500 m, (b) U200_BASE with finer grid cell of 200 m × 200 m, (c) the U200_BARRIER-barrier case, even the plume could not reach the top of the reservoir after 50 years injection compared with the (d) finer grid cell U200_BASE case.

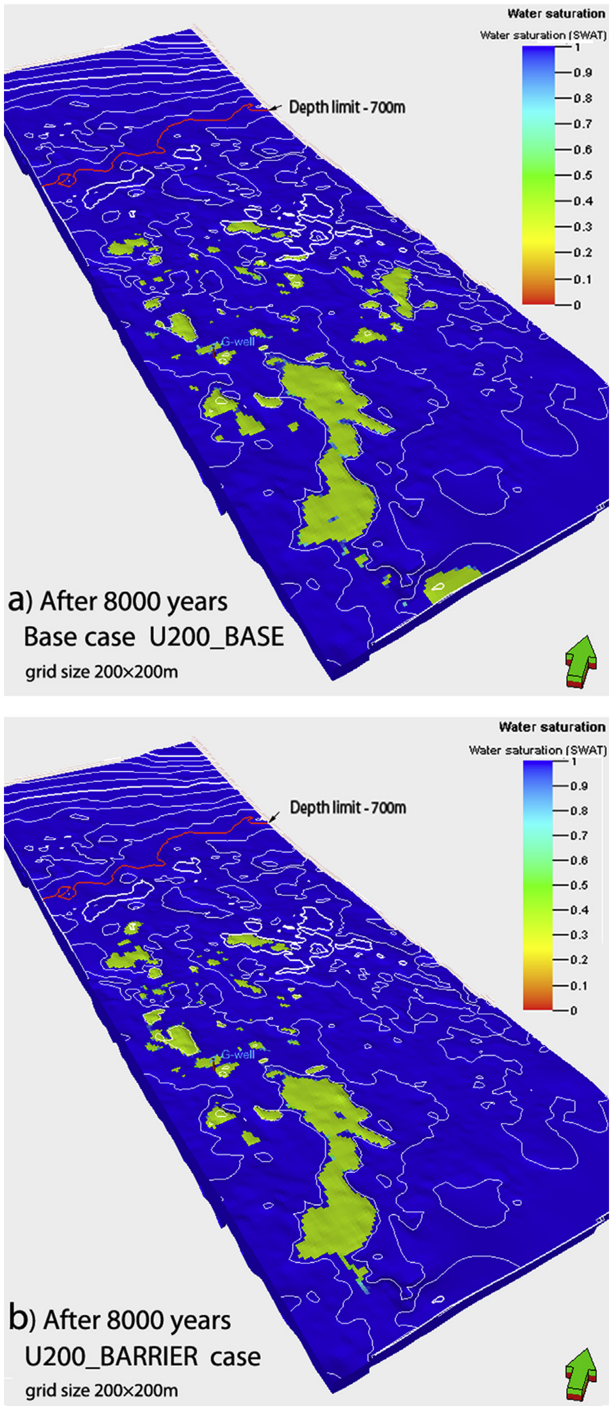

Fig. 7. The direction of the migration followed the topography, CO_2 fill up in surrounding local structures after about 8000 years after injection, (a) the base case U500 and (b) the U200_BARRIER-barrier case.

30 bars (ΔP: 30 bars), the constraint is higher than that in Utsira sand because Skade Formation is more consolidated than Utsira sand. The average reservoir pressure increases about 10 bars, Fig. 9.

The CO_2 plume covers over an area with diameter about 12 km at the end of 50 year injection in the base case S_BASE and the S_RELOCATION case with new location of injection well. The new well is near the area with some local sand injections observed in seismic (Fig. 10a and b). The result does not show that CO_2 migrates through small injection sand/local sand–sand connection with the S_RELOCATION case about 8000 year after injection. The CO_2 plume reaches the top of the reservoir very short after injection and also the border of the model after 350 years (Fig. 11a and b). The direction of the migration mainly followed the high topography. In this case local structures are very important to keep CO_2 stay and prevent it migrate further to the sector border/depth limit area.

The Skade Formation in our model represents only a small part of Skade Formation that connects to the shallower aquifer part in the west like mentioned in the geological overview part. The injectivity of the Skade sand will be affected by communication with the shallower part of the aquifer. By including the shallower aquifer part into the reservoir model, reservoir pressure increases only 3 bars and cumulative CO_2 volume is up to approximately152 Mt, Table 3 (approximately 85,000 million Sm^3, Fig. 9) after injection 50 years in S_AQUIFER case. However, with the shallower aquifer part included in the case S_AQUIFER, the spreading area of CO_2 plume is larger than without this part of the aquifer included (Fig. 11c and d).

The possibility of CO_2 migration through the mudstone layer which separate the two sands (Utsira and Skade) depends on the mudstone permeability. In the S_KTOP0 case with the highest permeability 0.1 mD and the highest relative vertical/horizontal permeability ratio ($K_v = K_h = 0.1$), CO_2 was able to penetrate through the mudstone to Utsira Formation above after about 1400 years (Fig. 12). In the other cases, S_KTOP00 ($K_h = 0.1$, $K_v/K_h = 0.1$), S_KTOP000 ($K_h = 0.1$, $K_v/K_h = 0.01$) and the S_BASE case ($K_h = 0.1$, $K_v/K_h = 0.001$), no CO_2 or very limited amount of CO_2 that could migrate through the mudstone layer.

4.3. CO_2 trapping mechanisms

In the Utsira fine grid case (U200_BASE), the total injected volume CO_2 was nearly 130 Mt (2.95×10^9 Kmol, in Fig. 13 equivalent to 67,000 million Sm^3, Fig. 5) of CO_2. CO_2 in the mobile CO_2 phase at the end of 50 years injection was 100 Mt (2.27×10^9 Kmol, Fig. 13). CO_2 trapped in gas phase (residual) was approximately 4.4 Mt (0.1×10^9 Kmol, Fig. 13). The amount of CO_2 in aqueous phase was estimated to be 25.6 Mt (0.58×10^9 Kmol, Fig. 13). The results showed that the CO_2 trapped by the dissolution trapping mechanism after 50 years injection period occupied a fraction of injected CO_2 of nearly 20%. CO_2 trapped in the residual trapping mechanism was estimated to around 3% and CO_2 trapped in the structural/stratigraphic trapping mechanism was approximately 77%. After 8000 years, the amount of CO_2 in aqueous phase becomes nearly 70%, residual trapping is less than 1% and mobile CO_2 decreases down to 29% of total CO_2 amount injected, Fig. 13. Corresponding to residual saturation of CO_2 equal to 0.02 (following relative permeability curves – [18]), CO_2 residual trapping is only 1%–3%.

If a residual saturation of CO_2 of 0.3 is assumed [33] and the corresponding imbibition curve is applied, CO_2 trapped by residual mechanism was increased during injection period end up at 35% at the end of 50 years injection. After injection stop, the amount of CO_2 trapped as residual gradually decreases and end up at 13% after 8000 years of post-injection (compare Fig. 13). The cause of the decrease of CO_2 residual from 35% to 13% after the injection finished could be due to the CO_2 trapped as residual mechanisms continues to dissolve in to the water, and the circulation of CO_2 unsaturated water replacing water saturated with CO_2 could maintain the dissolution process. The CO_2 in aqueous phase becomes nearly 75% and mobile CO_2 12% of total CO_2 amount injected after about 8000 years. The results showed that residual trapping is even more important if the sand has interbedded clay layers (or internal barriers) within the Utsira sand; see the case U200_BARR_HYS in Fig. 13.

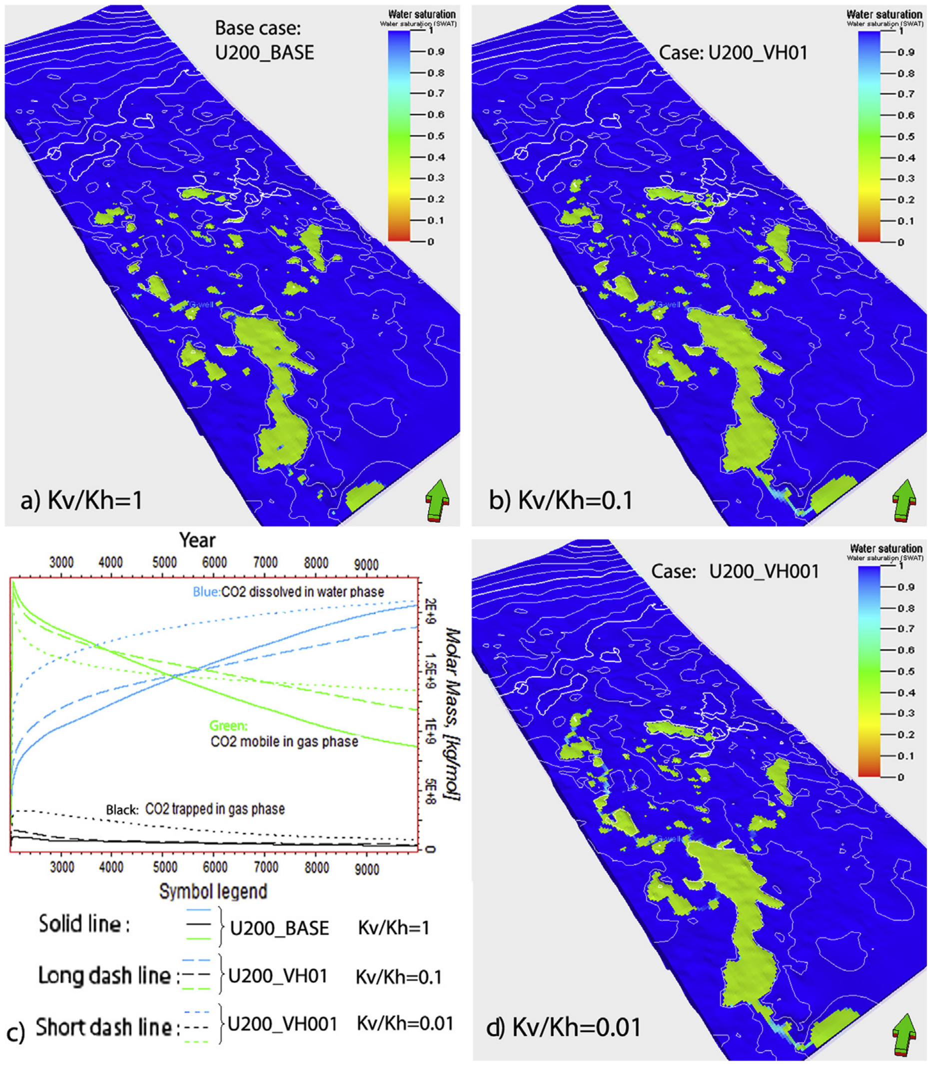

Fig. 8. Distribution of the CO_2 plume covers in larger area when sand has lower vertical permeability: (a) The base case (U200_BASE) with $K_v/K_h = 1$ homogenous sand, (b) The U200_VH01 case with $K_v/K_h = 0.1$ and (d) the U200_VH001 case of $K_v/K_h = 0.01$. (c) CO_2 amount in different trapping forms.

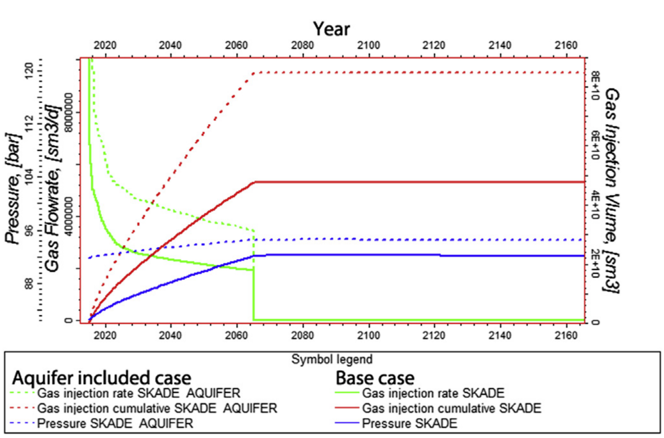

Fig. 9. Injection profile shows cumulative CO_2 volume injected in Skade Fm in two cases: the base case S_BASE without shallower aquifer included and S_AQUIFER with shallower aquifer included.

5. Discussion

5.1. Comparison with previous studies

Lindeberg et al., [15] estimated the storage capacity of the entire Utsira Formation to be between 20 and 60 Gt CO_2 in the aquifer with upper boundary to −500 m depths below mean sea level) by their simulation. The aquifer volume we consider suitable for storing CO_2 is deeper than 700 m. We also consider the risk of CO_2 migration to the west where the connectivity with very good sand in Upper Pliocene and Pleistocene units in the delta complex extend the aquifer up to shallow depths (200–300 m below sea level; Fig. 1a and b). As a result, our study estimates a smaller CO_2 storage capacity than [17]. In the Gestco report, over 42 Gt CO_2 is estimated to be stored in Utsira sand and the storage capacity of entire Skade Formation was estimated about 15 Gt [9]. However, these numbers were based on simple geological calculations, not simulations.

By exploring geological storage sites for CO_2 from Norwegian gas power plants for the Utsira South part [19], concluded that after 5000 years, 74% of the CO_2 should be dissolved into water and the remaining fraction immobilized Bergmo et al. (2009) also concluded that for suitable injection points, migration distances of

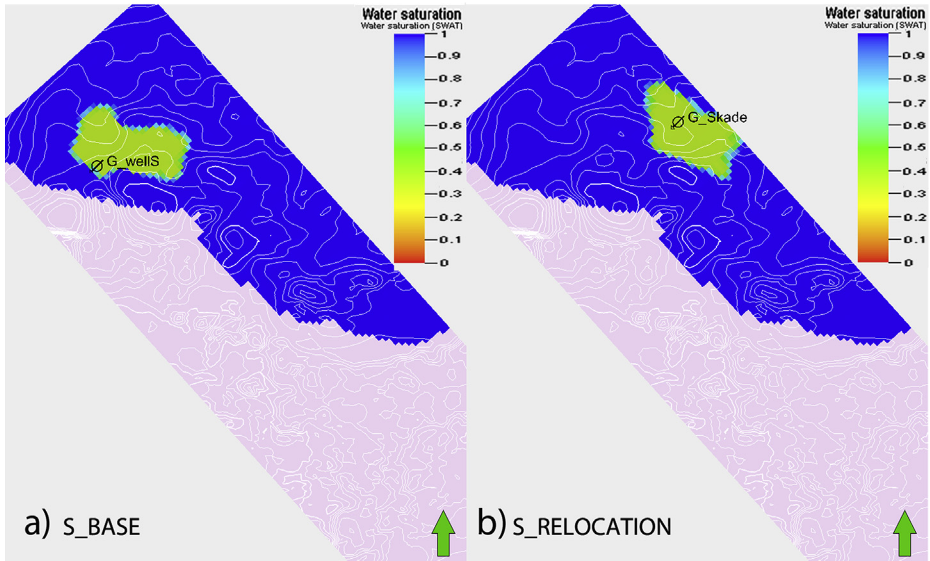

Fig. 10. The CO_2 plume distribution in Skade Fm after 50 years injection: (a) base case with the well further in the south and (b) another case with the injection well located near the area with thin Skade sand layer and area with some local sand injections observed in seismic.

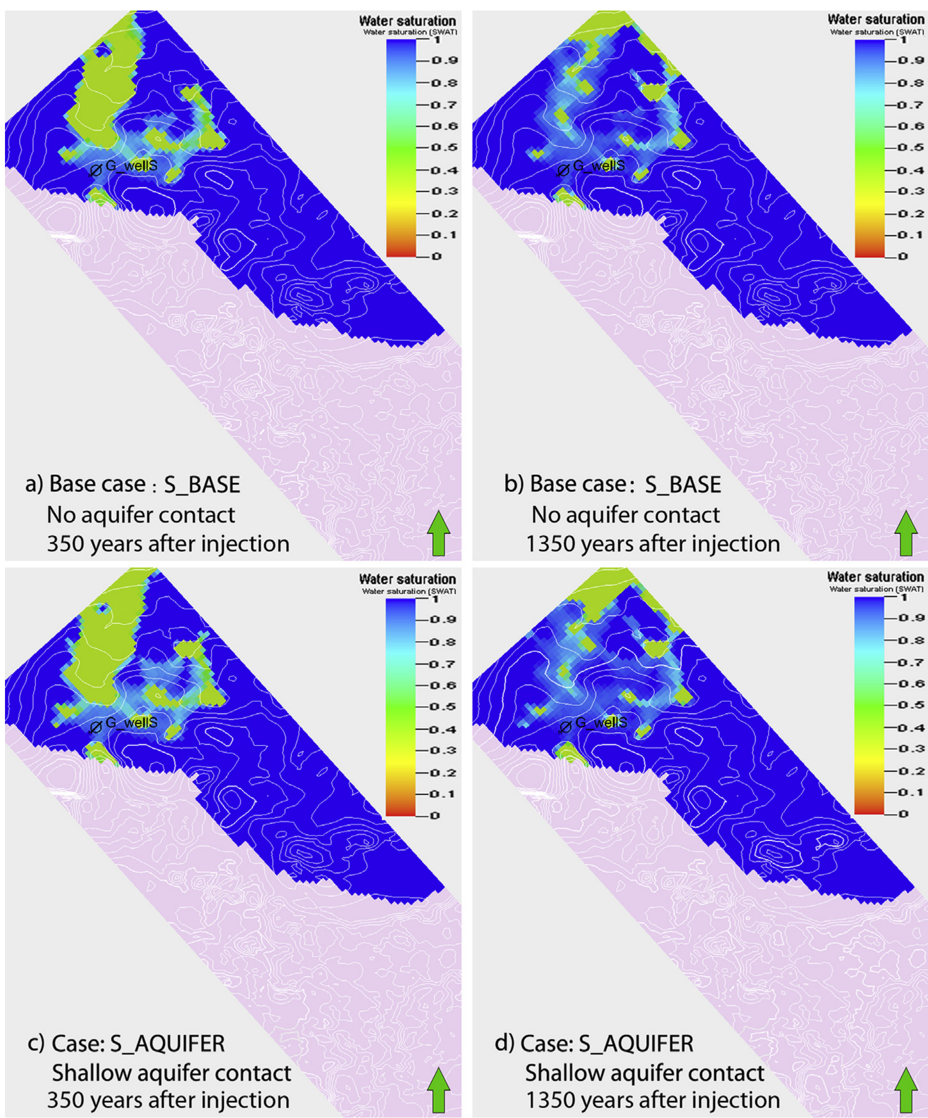

Fig. 11. The CO_2 plume reaches the top of the reservoir short after injection and also the border of the model/Norwegian sector after 350 years (a) base case and 1350 years, CO_2 plume reaches the model/Norwegian sector (b). The distribution area of CO_2 plume in the case without aquifer contact (a and b) is smaller than including aquifer contact (c and d).

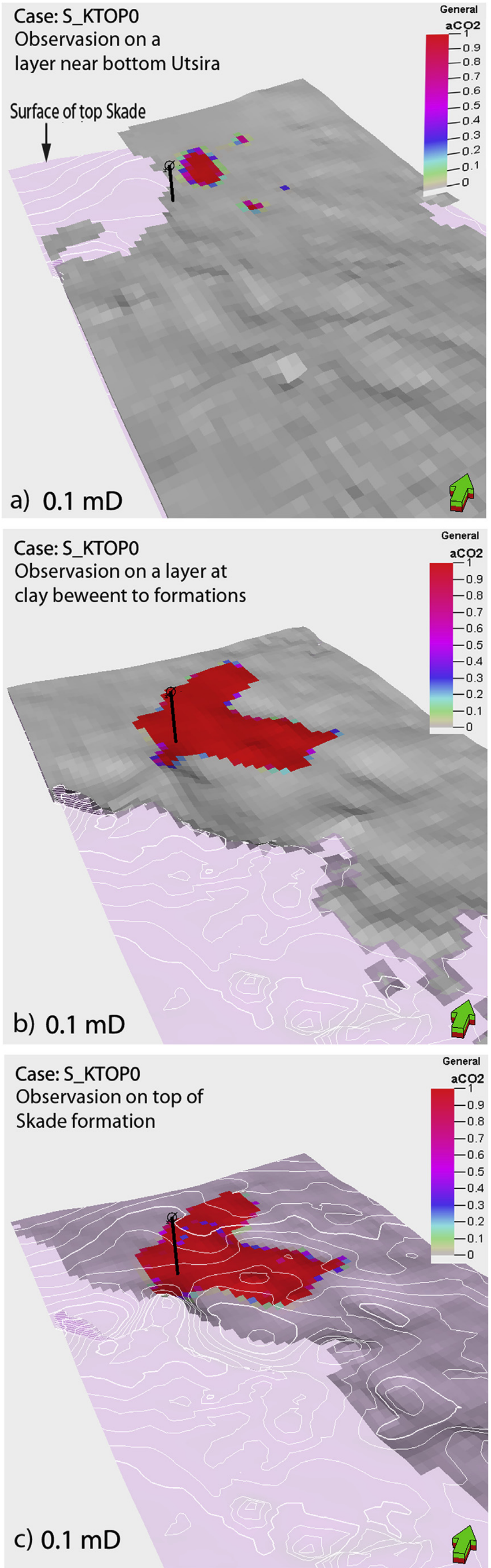

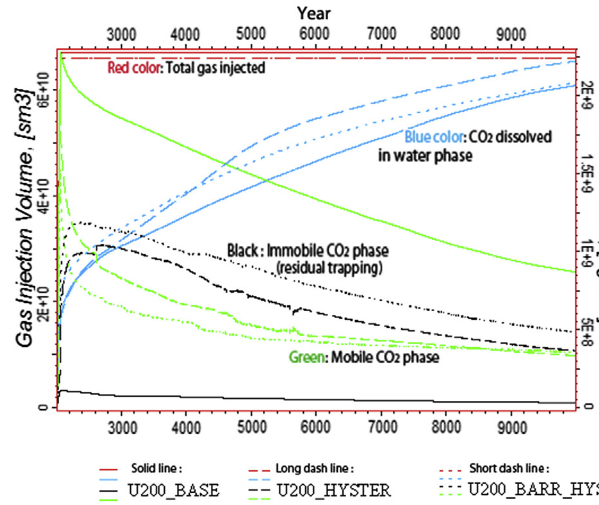

Fig. 13. CO_2 amount in mobile, immobile CO_2 phase and total CO_2 injection volume vs. time for CO_2 injection in Utsira Fm., U200_BASE is the base case with homogenous sand, U200_HYSTER was applied with imbibitions curve (hysteresis applied) and U200_BARR_HYS was applied with hysteresis and the sand with internal barriers (clay layers).

CO_2 plume could be up to 33 km from the injection point during a 5000 years period, and that there were no indications that it would migrate to any places where it may reach the shallow parts of the formation in the west [19]. The results in this study also confirm that about 70–75% of the CO_2 was dissolved into water after 8000 years (Fig. 14) and that the CO_2 plume could migrate 20 km away from the injection well (Fig. 7).

5.2. Model's uncertainties

This study is based on new stratigraphic studies and 3D seismic interpretation, and is considered to have reduced uncertainty compared to previous studies. However, uncertainties relating to the geological model, communication between to formations, as well as internal aquifer communication, and geological uncertainties of reservoir size remain. The assumptions for the reservoir properties of the injection area are considered to be on the conservative side in terms of porosity and permeability. The regional sealing capacity of the top seal is still regarded as one of the main uncertainties for large scale injection and storage in the Utsira-Skade aquifer. Nevertheless, the geological model was built based on seismic interpretation (from seismic cube) which cannot detect correctly reservoir properties of the rock. These properties are based on a limited number of drilled well in a large area. Moreover, the numerical model consist of thousands grid cells that have the dimensions from 50 × 50 m to 500 × 500 m and each cells contains only one value of a property, for example porosity, permeability and velocity (for depth conversion), by up scaling (averaging) process. The model cannot describe detailed feature of nature geological heterogeneity. The fraction of CO_2 in the brine solution is also deviated with different simulation-grid size and with the geological complex degree [34]. However, the dissolution of CO_2 can be accelerated by brine injection on top of free CO_2 cap to

Fig. 12. When vertical permeability in the mudstone/clay layer between two formations is 0.1 mD (or higher) in the case S_KTOP01, after 1400 years CO_2 could migrate up to Utsira Fm above. (a) Observation on a layer in Utsira sand and CO_2 present there, (b) Observation on a clay/mud stone layer which is between two formations, CO_2 present there. (c) Observation at top Skade Formation/sand.

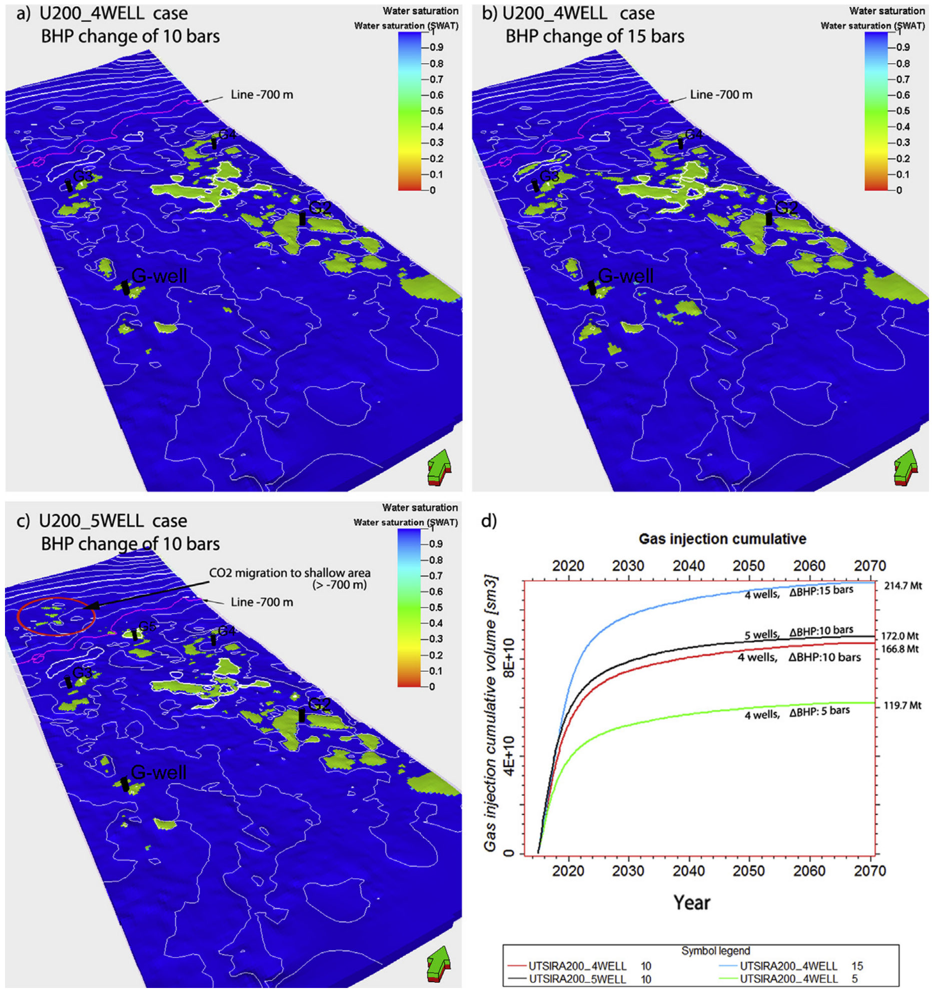

Fig. 14. CO_2 injection with 4 wells in the case U200_4WELL with different BHP changes of 10 bars (a) and 15 bars (b). The case 5U200_5WELL with 5 wells and with BHP change of 10 bars (c). Graph (d) shows the injected volume of CO_2 is affected significantly by BHP constraint, not by number of injection well.

increases the rate of solubility trapping in saline aquifers and therefore increases the security of storage [34]. In another hand, the reservoir with vertical heterogeneity in nature and tortuosity could limit vertically circulation and exchange of the water phase saturated with CO_2 and water under saturated with CO_2. But, anisotropy ratio (vertical horizontal permeability ratio), in contrast, shows that with low vertical anisotropy ratio of 0.01, the prevailing mechanism is lateral expansion of the injected CO_2 resulting in significantly higher dissolution [34]. A analytical method for fluid mixing in steady and transient buoyancy-driven flows induced by laminar natural convection in porous layers is presented in Ref. [35] and concentration of CO_2 can be correlated to velocity vector. But with turbulent flow with strong nonlinear interactions between density-driven instabilities that may happen in reservoirs, needs to be further investigated.

We are aware of that the different grid sizes create deviation of results. Due to the enormous area covered by the model and the computer capacity, the grid size of the model may not be smaller than 200 × 200 m.

Details about the communication within the huge Utsira/Skade aquifer are not yet mapped out. We have assumed that the communication between to formation-sands is around Utsira High [9]. Sand injections from Skade Formation into Utsira Formation were observed locally in seismic data. We are uncertain about the real communications and how much CO_2 may migrate into Utsira sand through this local sand–sand connection.

The simulation results in the present study have had the ambition to give a rough estimate of CO_2 trapped by different trapping mechanisms. However, more work is needed to access the uncertainties of the model that may affect the results and the accuracy of the calculations. There are very few studies about the multi-phase behavior of CO_2 supercritical and brine properly. The relative permeability curves used in this study were obtained from Ref. [18]. It is recommended to carry out more laboratory studies on multi-phase behavior of the fluids to obtain properly relative permeability curves for the dedicated site. These kinds of data are needed to improve further studies of the relative importance of trapping mechanisms and CO_2 storage capacity in saline aquifers. Furthermore, additional simulation studies should be carried out with pressure management, i.e. by including schemes of formation water extraction.

6. Summary

In Utsira Formations, study shows that ca. 170 Mt CO_2 could be injected in Utsira sand in the segment model with 4 horizontal wells in 50 years injection period, BHP change of 10 bars with no water production. Higher BHP constraint of 15 bars, CO_2 injected in the segment can be 215 Mt. Schemes of formation water extraction for pressure management should be focused more.

In Skade Formations, it is quite likely that CO_2 could quickly migrate to the west-north segment boundary due to the tilting of the top Skade surface. By communicating with the shallow aquifer part on the west, the migration distant of CO_2 will be further than the results shown in the Skade base cases, but with less pressure build-up.

The simulation results showed that the CO_2 trapped by the dissolution trapping mechanism occupied a fraction of approximately 20% of the injected CO_2. CO_2 trapped in the residual trapping mechanism is approximately3% and CO_2 trapped in the structural/stratigraphic trapping mechanism more or less 77% at the end of 50 years of injection. After about 8000 years after the injection period, the dissolved amount increase to nearly 70%, and residual trapping decreases to approximately 1%, while, mobile CO_2 decreased down to 29% of the total CO_2 amount injected. These results were obtained by applying with residual saturation of CO_2 equal to 0.02. Thus, CO_2 residual trapping is 3% (at the end 50 years of injection) and decreasing to 1% after 8000 years. However, if residual saturation of CO_2 equals to 0.3, the CO_2 trapped by residual mechanism will be higher, 35% (at the end 50 years of injection) and decreasing to 13% after 8000 years. Mobile CO_2 will be reduced in this case.

Acknowledgments

Authors greatly acknowledge all the colleagues in NPD helping us to finish this study and the useful discussions that help to improve this paper. We are grateful to thank Robert William for the help to correct the language in this article.

References

[1] Holloway S. Underground sequestration of carbon dioxide—a viable greenhouse gas mitigation option. Energy 2004;30:2318–33.
[2] Holloway S. Storage of fossil fuel-derived carbon dioxide beneath the surface of the earth. Annual reviews of Energy and the Environment 2001;26: 145–66.
[3] Bachu S, Bonijoly D, Bradshaw J, Burruss R, Holloway S, Christensen NP, et al. CO_2 storage capacity estimation: methodology and gaps. International Journal of Greenhouse Gas Control 2007;1:430–43.
[4] Benson SM, Cole DR. CO_2 sequestration in deep sedimentary formations. Elements – An International Magazine of Mineralogy, Geochemistry, and Petrology 2008.
[5] Torp TA, Gale J. Demonstrating storage of CO_2 in geological reservoirs: the Sleipner and SACS projects. Energy 2004;29.
[6] Maldal T, Tappel IM. CO_2 underground storage for Snøhvit gas field development. Energy 2004;29.
[7] Halland EK, Gjeldvik IT, Johansen WT, Magnus C, Meling IM, Pedersen S, et al. CO_2 atlas Norwegian north sea. Norwegian Petroleum Directorate; 2011.
[8] Eiken O, Ringrose P, Hermanrud C, Nazarian B, Torp TA, Høier L. Lessons learned from 14 years of CCS operations: Sleipner, in Salah and Snøhvit. Energy Procedia 2011;4:5541–8.
[9] Bøe R, Magnus C, Osmundsen PT, Rindstad BI. CO_2 point sources and subsurface storage capacities for CO_2 in aquifers in Norway. NGU Report 2002.10 2002132.
[10] Gregersen U, Johannessen PN. Distribution of the Neogene Utsira Sand and the succeeding deposits in the Viking Graben area, North Sea. Marine and Petroleum Geology 2007;24:591–606.
[11] Eidvin T, Rundberg Y. Post-Eocene strata of the southern Viking Graben, northern North Sea; integrated biostratigraphic, strontium isotopic and lithostratigraphic study. Norwegian Journal of Geology 2007;87:391–450.
[12] Estublier A, Lackner AS. Long-term simulation of the Snohvit CO_2 storage. 9 1. Greenhouse Gas Control Technologies; 20093221–8.
[13] Pham VTH, Maast TE, Hellevang H, Aagaard P. Numerical modeling including hysteresis properties for CO_2 storage in Tubåen formation, Snøhvit field, Barents Sea. Energy Procedia 2011;4:3746–53.
[14] Eigestad GT, Dahle HK, Hellevang B, Riis F, Johansen WT, Oian E. Geological modeling and simulation of CO_2 injection in the Johansen formation. Computational Geosciences 2009;13:435–50.
[15] Lindeberg E, Bergmo P. The long-term fate of CO_2 injected into an aquifer. In: Proceedingsvols. I and Ii. Greenhouse Gas Control Technologies; 2003. p. 489–94.
[16] Lindeberg E, Zweigel P, Bergmo P, Ghaderi A, Lothe A. Prediction of CO_2 distribution pattern improved by geology and reservoir simulation and verified by time lapse seismic. Greenhouse Gas Control Technologies; 2001372–7.
[17] Lindeberg E, Vuillaume J-F, Ghaderi A. Determination of the CO_2 storage capacity of the Utsira formation. Energy Procedia 2009;1:2777–84.
[18] Singh V, Cavangh A, Hansen H, Nazarian B, Iding M, Ringrose P. Reservoir modeling of CO_2 plume behavior calibrated against monitoring data from Sleipner. Norway: Society of Petroleum Engineers; 2010.
[19] Bergmo PES, Grimstad A-A, Lindeberg E, Riis F, Johansen WT. Exploring geological storage sites for CO_2 from Norwegian gas power plants: Utsira South. Energy Procedia 2009;1:2953–9.
[20] Pham VTH, Lu P, Aagaard P, Zhu C, Hellevang H. On the potential of CO_2-water-rock interactions for CO_2 storage using a modified kinetic model. International Journal of Greenhouse Gas Control 2011;5:1002–15.
[21] Johnson JW, Nitao JJ, Knauss KG. Reactive transport modelling of CO_2 storage in saline aquifers to elucidate fundamental processes, trapping mechanisms and sequestration partitioning. In: Baines SJ, Worden RH, editors. Geological storage of carbon dioxide. Geological Society, Special Publications; 2004. p. 107–28.
[22] Audigane P, Gaus I, Czernichowski-Lauriol I, Pruess K, Xu T. Two-dimensional reactive transport modeling of CO_2 injection in a saline Aquifer at the Sleipner site, North Sea. American Journal of Science 2007;307:974–1008.
[23] Thibeau S, Nghiem LX, Ohkuma H. A modeling study of the role of selected minerals in enhancing CO_2 mineralization during CO_2 aquifer storage. In: SPE annual technical conference and exhibition, 11–14 Nov 2007, California, USA; 2007.
[24] Aagaard P, Hellevang H, Pham VTH. On the potential for secondary carbonate growth in sedimentary basins. In: 21st V.M. Goldschmidt conference, August 14–19, Prague, Czech Republic; 2011.
[25] Isaksen D, Tonstad K. A revised cretaceous and tertiary lithostratigraphic nomenclature for the Norwegian North Sea, vol. 5. NPD Bulletin; 198965.
[26] Eidvin T, Rundberg Y, Smelror M. Revised chronology of Neogene sands (Utsira and Skade formations) in the central and northern North Sea. In: Hurst A, editor. Onshore – offshore relationships on the North Atlantic margin. Trondheim: Norwegian Geology Society (NGF) and Norwegian Petroleum Society (NPF) Conference; 2002.
[27] Gregersen U, Michelsen O, Sørensen JC. Stratigraphy and facies distribution of the Utsira formation and the Pliocene sequences in the northern North Sea. Marine and Petroleum Geology 1997;14:893–914.
[28] Zweigel P, Arts R, Lothe AE, Lindeberg EBG. Reservoir geology of the Utsira formation at the first industrial-scale underground CO_2 storage site (Sleipner area, North Sea), vol. 233. Geological Society, London, Special Publications; 2004165–80.
[29] Chadwick RA, Zweigel P, Gregersen U, Kirby GA, Holloway S, Johannessen PN. Geological reservoir characterization of a CO_2 storage site: the Utsira sand, Sleipner, northern North Sea. Energy 2004;29:1371–81.
[30] Egeberg PK, Aagaard P. Origin and evolution of formation waters from oil fields on the Norwegian shelf. Applied Geochemistry 1989;4:131–42.
[31] Spycher N, Pruess K, Ennis-King J. CO_2–H_2O mixtures in the geological sequestration of CO_2. I. Assessment and calculation of mutual solubilities from 12 to 100 °C and up to 600 bar. Geochimica Et Cosmochimica Acta 2003;67: 3015–31.
[32] Spycher N, Pruess K. A phase-partitioning model for CO_2-brine mixtures at elevated temperatures and pressures: application to CO_2-enhanced geothermal systems. Transp Porous Med. Springer; 2009.
[33] Bennion DB, Bachu S. Drainage and imbibition relative permeability relationships for supercritical CO_2/brine and H_2S/brine systems in intergranular sandstone, carbonate, shale, and anhydrite rocks. SPE Reservoir Evaluation & Engineering 2008;11:487–96.
[34] Hassanzadeh H, Pooladi-Darvish M, Keith DW. Accelerating CO_2 dissolution in saline aquifers for geological storage, mechanistic and sensitivity studies. Energy & Fuels 2009;23:3328–36.
[35] Meybodi HE, Hassanzadeh H. Mixing induced by buoyancy-driven flows in porous media. AIChE Journal 2012.